



An experimental study of the thermal performance of a novel photovoltaic double-skin facade in Hong Kong

Jinqing Peng, Lin Lu^{*}, Hongxing Yang

Renewable Energy Research Group (RERG), Department of Building Services Engineering, The Hong Kong Polytechnic University, Hong Kong, China

Received 20 May 2013; received in revised form 7 August 2013; accepted 21 August 2013

Available online 16 September 2013

Communicated by: Associate Editor Matheos Santamouris

Abstract

Ventilated building-integrated photovoltaic (BIPV) facades can not only generate electricity at the locations of buildings themselves but if designed optimally, such facades can also reduce the respective heat gains and heat losses in summer and winter via the building envelope. The development of a novel ventilated BIPV double-skin facade (DSF), constituted by a see-through amorphous silicon (a-Si) PV module and an inward opening window, is reported in this paper. In order to enhance ventilation, an air-flow duct, 400 mm in depth is situated between the outside PV module and the inside window. This ventilation design can remove much of the waste heat generated by the PV module energy conversion processes, and thus bring down the operating temperature of the solar cells. Infrared thermal imaging was adopted in relation to the ventilated PV-DSF to visually demonstrate this ventilating effect. It was found that the air temperature at the outlet louver is higher than that at the inlet louver by 2.2–2.3 °C. The thermal performance of PV-DSFs operating in different modes was studied and compared. The results showed that the ventilated PV-DSF provides the lowest solar heat gain coefficient (SHGC), while the non-ventilated PV-DSF better reduces heat loss. Based on the experimental results, the optimum operation strategy for the PV-DSF under different weather conditions has been determined and proposed. This novel PV-DSF is more suitable for sub-tropical climates because it results in a much lower SHGC than that of a low-e coating DSF.

© 2013 Elsevier Ltd. All rights reserved.

Keywords: Building-integrated photovoltaic; See-through amorphous silicon; Solar heat gain coefficient; Building energy efficiency

1. Introduction

In 2010, about 61% of the total electricity end-uses were consumed by buildings in Hong Kong and this proportion has increased over recent years. Among the various types of building energy use, space air-conditioning has accounted for more than 50% (Hong Kong EMSD, 2012). The large amount of air-conditioning energy consumption can be partially attributed to the extensive use of glass curtain walls currently used in modern buildings. The solar heat gains and heat losses via glass curtain walls share a large portion of office building air conditioning loads. Hence the need to develop new types of glass curtain

walls is apparent. Such walls need to meet the aesthetic demand and also reduce the transmission of heat gains/losses. Advanced facade system developments, involving double skin facade (DSF) technologies, have been attracting growing attention due to their improved thermal insulation performance (Gratia and Herde, 2004, 2007; Safer et al., 2005; Jiru et al., 2011; Zöllner et al., 2002; Zhou and Chen, 2010; Manz and Frank, 2005). A ventilated double-skin facade using both external and internal clear glass can significantly reduce solar heat gain through the building envelope. An annual cooling load reduction of up to 26% greater than that achieved by the use of a single-glazed curtain wall can be attained by this kind of DSF system in Hong Kong (Haase and Amato, 2006). Similarly, a DSF system, with a single clear glass inner pane and double reflective glass outer pane, can also reduce the annual cool-

^{*} Corresponding author. Tel.: +852 3400 3596; fax: +852 2765 7198.
E-mail address: bellu@polyu.edu.hk (L. Lu).

Nomenclature

Abbreviation

| | |
|-------------------|----------------------------------|
| AC | air conditioning |
| a-Si | amorphous silicon |
| ambient T | ambient temperature |
| c-Si | crystalline silicon |
| DC | direct current |
| DSF | double skin facade |
| indoor T | temperature of indoor room |
| inner surface T | temperature of the inner surface |
| low-e | low-emission |
| natural-V | natural-ventilated |
| non-V | non-ventilated |
| PMV | predicted mean vote |
| PV | photovoltaic |
| PV module T | temperature of the PV module |
| PV-DSF | photovoltaic double-skin facade |
| SHGC | solar heat gain coefficient |
| STC | standard testing conditions |
| TMY | typical meteorological year |
| WWR | window wall ratio |

Subscripts

| | |
|-----------------|---|
| G_i | solar radiation incident on the south-facing vertical PV-DSF (W/m^2) |
| G_r | solar radiation reflected by the surfaces of the tempered glass layers (W/m^2) |
| E_{pv} | power output of the see-through a-Si PV module (W/m^2) |
| G_{cells} | energy absorbed by the solar cells but dissipated as waste heat (W/m^2) |
| $G_{a-glasses}$ | energy flows absorbed by the tempered glass layers and the clear glass (W/m^2) |
| G_{shg} | solar heat gain of the indoor room (W/m^2) |
| G_{rad} | radiative heat flows occurring between the PV module and the ambient environment as well as between the inside window and the indoor room (W/m^2) |
| G_{conv} | convective heat flows occurring at each surface of the PV module and the window (W/m^2) |
| G_{cap} | rates of internal energy increase of the PV module, the window layer and the air flow (W/m^2) |
| G_{exh} | air flow heat exhaust rate between the PV module and the inward opening window (W/m^2) |

ing load by 26% when compared with that of a conventional single-skin facade with absorptive glazing (Chan et al., 2009). Although an air-tight DSF reduces heat losses in winter, the ventilated DSF is even more suitable for buildings in subtropical climates found in such as Hong Kong. The airflow in the DSF significantly reduces the heat gain and therefore building cooling loads for most of the year.

Additionally, a ventilated DSF integrated with photovoltaic (PV) glazing not only can reduce the energy use of air-conditioning and artificial lighting, but also generate electricity in situ. Thus, much research has focused on the energy performance of PV window or facades in recent years (Radhi, 2010; Wang et al., 2006; Yun et al., 2007; Han et al., 2010, 2013; Park et al., 2010; Peng et al., 2013; Charron and Athienitis, 2006; Infield et al., 2004). Miyazaki et al. (2005) investigated the thermal performance of a PV window, consisting of two layers of glass with a see-through amorphous silicon (a-Si) solar cell placed between the layers. The simulation results using *EnergyPlus* showed that, compared with single-glazed and double-glazed windows, using PV windows with a window wall ratio (WWR) of 50% reduced the total energy use (including the electricity used for cooling, heating and lighting) by 23% and 16.4% respectively. Chow et al. (2010) reviewed the energy performance of various advanced window technologies, including a series of single-glazed windows and double-glazed windows. For single-glazed windows, the simulation results showed that

PV laminated glass provided the best solar heat gain coefficient (SHGC) compared with clear glass and the low-e coating glass. However, the low-e glass had a lower U-value than that of the PV laminated glass because of its lower infrared emissivity properties. Similar results were found for corresponding double-glazed windows. Compared with double-glazed clear glass and low-e glass windows, the double-glazed PV glass window reduced room heat gain by 200% and 53%, respectively. The SHGCs of the single-glazed and double-glazed PV laminated windows were 0.28 and 0.177, respectively, which are far less than those found for the clear glass windows. Based on the above findings, it can be concluded that PV laminated windows are more suitable for use in subtropical climate conditions and the low-e glass windows in cold climate conditions.

A comparative study investigated the energy performance of double-glazed, single-glazed, force-ventilated and naturally-ventilated PV glazed windows (Chow et al., 2009b). It was reported that on a typical summer day, air conditioning energy consumption could be reduced by 26% and 61% by respectively using single-glazed and naturally-ventilated PV windows instead of a normal absorptive-glazed window. He et al. (2011) conducted an experimental study on the thermal performance of a PV double-glazed window and a PV single-glazed window. For the PV double-glazed window, the external layer was an a-Si PV panel and the internal layer was clear glass. Openings were provided at the

top and the bottom of the external layer. The study showed that the average total heat gain and secondary heat gain (including convective and infrared radiative heat transfer) of the PV double-glazed window were 78.3 W and 51.8 W, respectively, and accounted for only 53.5% and 45.8% of the PV single-glazed window heat gain. The authors explained that the better thermal performance of the PV double-glazed window was due to the ventilation openings at the top and bottom of the external layer, which contributed to heat extraction. The experimental data also indicated that it is the secondary heat gain from the window which dominates the total heat gain. The thermal comfort index of these two PV windows was evaluated using the predicted mean vote technique (PMV). It was found that the PV double-glazed window provided better thermal comfort than the PV single-glazed window due to the much lower inner surface temperature.

The overall energy performance of a ventilated PV window to be used in office buildings was evaluated (Chow et al., 2007). It was found that see-through a-Si glazing was more aesthetically and optically pleasing in the working environment than opaque crystalline silicon (c-Si) glazing. A comprehensive model including the energy balance, heat transfer as well as the optical performance of the ventilated PV window was developed by the authors. The simulation results based on the net energy provision by the PV modules and energy saving in artificial lighting and air conditioning, indicated that an optimum ventilated PV window of 2 m (W) × 1.5 m (L) could save up to an annual total of 800 kWh electricity in Hong Kong. The impact of naturally-ventilated PV glazing on air-conditioning load reduction has been reported by Chow et al., 2009a. The annual simulation results, based on the weather data of a typical meteorological year (TMY) in Hong Kong, showed that when compared to a common absorptive glazing, the use of naturally-ventilated PV glazing could reduce the air-conditioning energy use by 28%.

Although much research regarding advanced window and facade technologies has been reported, little experimental work has been conducted on the thermal performance of real double-skin facades with PV integrated glazing (PV-DSF). The study presented in this paper proposes a novel PV-DSF system, consisting of a see-through a-Si PV module and an inward opening window. This PV-DSF system not only generates electricity in situ but also can significantly reduce solar heat gain in summer and heat loss in winter. The thermal performance of PV-DSFs operating in different ventilated, naturally-ventilated and non-ventilated modes is analyzed and compared. Based on the experimental results, an optimum operational strategy for this PV-DSF system is recommended. The experimental results can also provide guidance towards the optimum design of future PV-DSF systems.

2. System description

Building facades are one of the main sources of the air-conditioning load. Poor insulation performance results in high cooling/heating energy use. To reduce building energy consumption, a novel PV double-skin facade (DSF) was developed in this study. This PV-DSF system consists of a double-glazed see-through a-Si PV module, an inward opening window as well as an air-flow duct between the two layers, as demonstrated in Fig. 1. The important structural parameters of this PV-DSF system are presented in Table 1. Besides generating power, this PV-DSF system also has better thermal insulation performance.

Because the front and back covers consist of tempered glass layers and the a-Si layers are very thin, this double-glazed a-Si PV module is see-through and people inside the room can see the outdoor scenery. The inside layer of this PV-DSF unit can be inwardly opened and the indoor air can exchange with the outdoor fresh air when needed. In addition, during the daytime in winter, any sun warmed air in the air-flow duct can be released into the room by opening the inside window, thereby reducing, or even avoiding, the need for additional heating. In order to increase ventilation, two air ducts of depth 400 mm exist between the outside PV modules and the inside windows. These two air ducts are separated by a vertical insulation board, centrally located, to ensure that they do not affect each other when operating in different modes. Respective air inlet and outlet louvers are installed below and above the PV modules. All the above elements constitute the novel ventilated PV-DSF system. Cold air enters the air-flow duct from the bottom inlet louver, exchanges heat with the PV module and exhausts a considerable amount of waste heat via the upper outlet louver. The greatest advantage of this design is that the ducted air flow is able to remove much waste heat and reduce the operating temperature of the solar cells.

3. Energy flows analysis

Although the structure of the ventilated PV-DSF system is simple, its energy conversion and the heat transfer processes are complicated. Fig. 2 presents the energy flows and the heat transfer processes in detail. The solar radia-

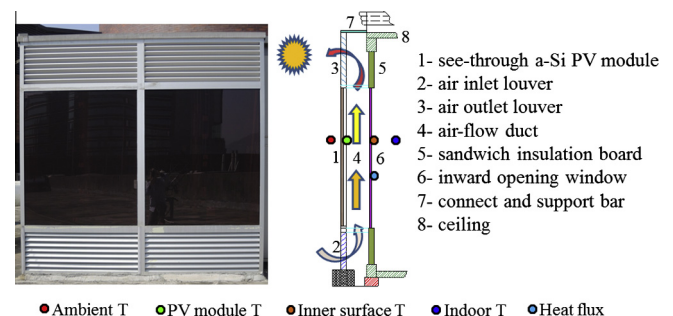


Fig. 1. The structure of the ventilated PV-DSF system.

Table 1
The important structural parameters of the ventilated PV-DSF system.

| Parameters | Value |
|------------------------|---------|
| Width of PV module | 1.1 m |
| Height of PV module | 1.3 m |
| Thickness of PV module | 0.006 m |
| Width of louver | 1.1 m |
| Height of louver | 0.5 m |
| Depth of air flow duct | 0.4 m |
| Window wall ratio | 0.4 |

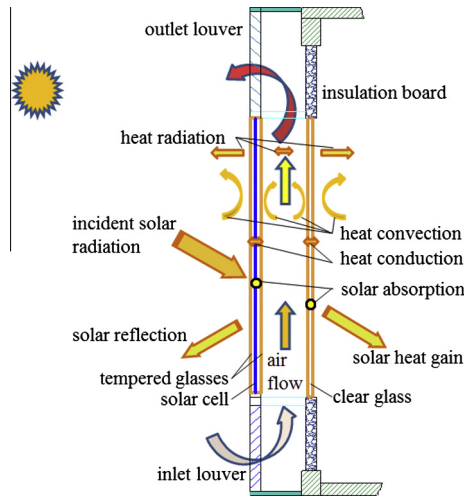


Fig. 2. Energy flows and heat transfer in the ventilated PV-DSF system.

tion incident on the south-facing vertical PV module is partly reflected by the tempered glass layers and partly absorbed by the a-Si solar cell layers. The remainder of the incident solar radiation passes through the PV module and enters the indoor room providing solar heat gain. The solar energy absorbed by the a-Si solar cells is partly converted into direct current (DC) electricity (only about 6–8% is converted into electricity in a see-through a-Si PV module) and the absorbed remainder, is dissipated as waste heat, resulting in an increase of the PV module operating temperature. The waste heat from the solar cell layer is conducted within the front and back tempered glass layers. The air-flow in the duct exchanges heat with the back side tempered glass layer and the front side of the window in the form of heat convection and is then exhausted via the upper outlet louver. In addition, the PV module and the inside window also exchanges heat with the surrounding objects by convection and long wave radiation. The energy balance equation of the ventilation PV-DSF is given by:

$$G_i = G_r + E_{pv} + G_{cells} + G_{a-glasses} + G_{shg} + G_{rad} + G_{conv} + G_{cap} + G_{exh} \quad (1)$$

where G_i is the solar radiation incident on the south-facing vertical PV-DSF; G_r is the solar radiation reflected by the surfaces of the tempered glass layers; E_{pv} is the power output of the see-through a-Si PV module. The latter has an

energy conversion efficiency of 6.6% under standard testing conditions (STC); G_{cells} is the energy absorbed by the solar cells but not converted into electricity and dissipated as waste heat; $G_{a-glasses}$ are the energy flows absorbed by the tempered glass layers and the clear glass; G_{shg} is the solar heat gain of the indoor room, which is closely related to the absorptivity of the PV module and the transmittivities of the tempered glass layers; G_{rad} are the radiative heat flows occurring between the PV module and the ambient environment as well as between the inside window and the indoor room; G_{conv} are the convective heat flows occurring at each surface of the PV module and the window; G_{cap} are the rates of internal energy increase of the PV module, the window layer and the air flow; and G_{exh} is the air flow heat exhaust rate between the PV module and the inward opening window.

4. Experimental methodology

The studied PV-DSF system can operate under different modes by opening or closing the inlet and outlet louvers. As shown in Figs. 3 and 4 types of operation modes were achieved by opening or closing different inlet and outlet louvers. The focus of the study presented in this paper is mainly on the experimental study of the thermal performance of the PV-DSF operating under different ventilation modes: (a) ventilated, (b) natural-ventilated and (c) non-ventilated. In Fig. 3, the left PV module is denoted as PV Module 1 with its corresponding inside window as Window 1; the right PV module is denoted as PV Module 2 with its corresponding inside window as Window 2. The specific experimental procedures and objectives of the different modes are summarized in Table 2. From Fig. 3 and Table 2, it can be seen that the objective of Mode 1 is to investigate

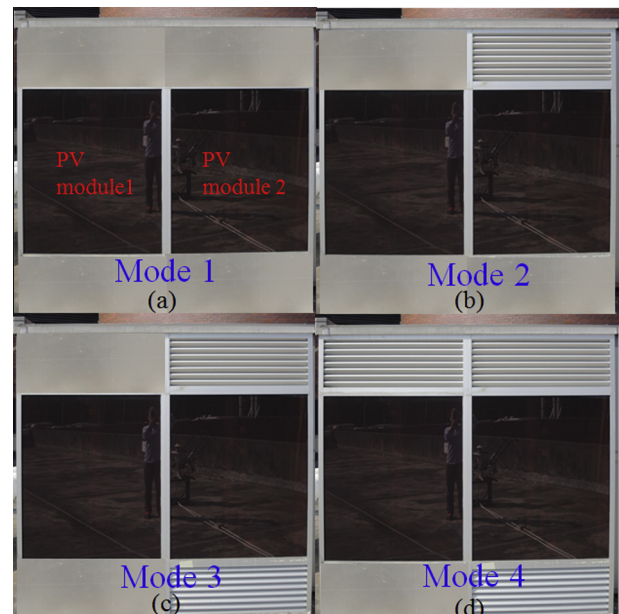


Fig. 3. The different operating modes of the novel PV-DSF system.

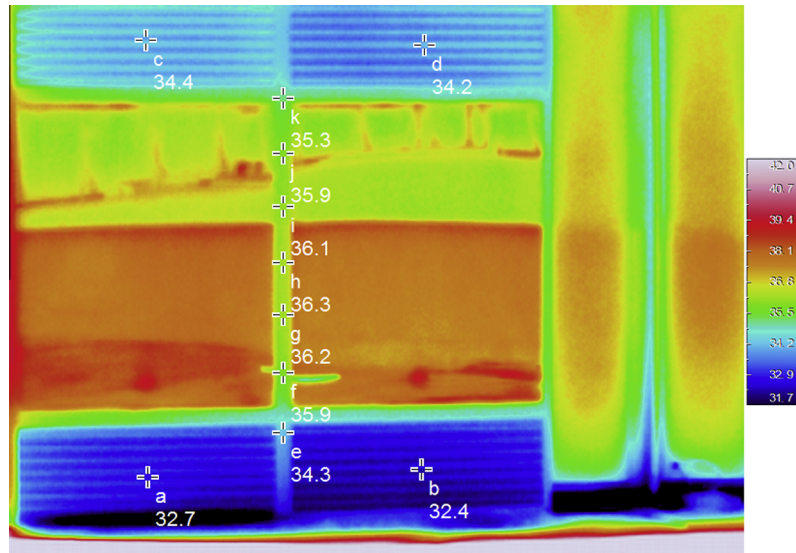


Fig. 4. The infrared thermal imaging of the ventilated PV-DSF system.

Table 2
The specific operating procedures and objectives of different modes of the PV-DSF.

| Operation modes | Objectives | Specific operating procedures |
|-----------------|--|--|
| Mode 1 | Investigate the passive heating effect of PV-DSF in winter | Close all inlet and outlet louvers and open the inward windows; turn off the air-conditioning |
| Mode 2 | Comparative study of the thermal performance of PV-DSFs operating under non-ventilated and naturally-ventilated conditions | Close all inlet and outlet louvers except the right outlet louver; close the inward windows; turn on the indoor air-conditioning and maintain the air temperature at 22 °C |
| Mode 3 | Comparative study of the thermal performance of PV-DSFs operating under ventilated and non-ventilated conditions | Close the inlet and outlet louvers on the left and open the louvers on the right; (the other operations are the same as for Mode 2) |
| Mode 4 | Comparative study of the thermal performance of PV-DSFs operating under ventilated and naturally-ventilated conditions | Open all inlet and outlet louvers except the left inlet louver; (the other operations are same as for Mode 2) |

the passive heating effect of PV-DSF in winter, while that of Modes 2–4 is to compare the thermal performance of PV-DSF operating under non-ventilated, naturally-ventilated and ventilated conditions. The experiment was conducted from Jan. 2013 to Feb. 2013 in Hong Kong. Equipment such as pyranometers, thermocouples, heat flux meters, infrared thermal imager as well as weather station were used for recording the ambient temperature, solar

radiation, various temperatures as well as heat gains and heat losses. The locations of these sensors are marked in Fig. 1 and their specifications are listed in Table 3. Except for the signals of the weather station, all the other sensors' signals were recorded by a GL820 Midi Data Logger at a time interval of 1 min. The GL820 Midi Data Logger can accept voltage (from 20 mV to 50 V), temperature, humidity, pulse and logic signals. The weather station data, such

Table 3
The key experimental equipment and their specifications.

| Experimental equipment | Manufacturer and model | Sensitivity and/or technical data | Measurement error |
|-------------------------|-------------------------------------|---|---|
| Pyranometer | EKO instruments (MS-802) | 6.91 $\mu\text{V}/(\text{W}/\text{m}^2)$ | Non-linearity <0.2% (at 1000 W/m^2) $\pm 0.5\text{ }^\circ\text{C}$ |
| Thermocouples | RS components (T type thermocouple) | Temperature range: -50 to $400\text{ }^\circ\text{C}$ | |
| Heat flux meters | Captec Enterprise (HS-30) | 2.5 $\mu\text{V}/(\text{W}/\text{m}^2)$; Response time: 0.3 s | <3% |
| Infrared thermal imager | NEC (R300SR) | Thermal Resolution <0.05 K at 60 Hz and $30\text{ }^\circ\text{C}$; Temperature range: -40 to $120\text{ }^\circ\text{C}$ | $\pm 1\text{ }^\circ\text{C}$ or $\pm 1\%$ of reading |
| Data logger | Graphtec (GL820 Midi Data Logger) | Accepts voltage (20 mV to 50 V), temperature, humidity, pulse and logic signals | Minimum resolutions are 1 μV and $0.1\text{ }^\circ\text{C}$ |

as wind speed, wind direction, ambient temperature, humidity and global solar radiation, were independently collected by a data logger manufactured by Thies Clima.

For each operation mode, the experimental results were collected continuously for 3 days. For example, the experiment of Mode 2, for comparing the thermal performance of PV-DSF operating under non-ventilated and naturally-ventilated conditions, was conducted from 12:00 AM of 22 Jan. to 12:00 AM of 25 Jan. During this experimental period, the heat gains and heat losses as well as the temperatures of PV modules and indoor rooms of the non-ventilated and naturally-ventilated PV-DSFs were measured simultaneously under the same weather conditions. In order to verify the ventilation effect, a NEC infrared thermal imager (R300SR) was used for the imaging of the ventilated PV-DSF system. As shown in Fig. 4, the air temperature at the outlet louver is higher than that at the inlet louver by 2.2–2.3 °C, which indicates that the airflow is successfully removing heat from the PV modules and thereby enhancing their energy conversion efficiency into electricity. The ventilation simultaneously reduces the solar heat gain of the PV-DSF unit in summer, such that the air-conditioning energy consumption is reduced.

5. Results and discussion

In order to find an optimum operating strategy to maximize the overall energy efficiency of the PV-DSF system, the thermal performance, based mainly on the various temperature profiles, heat gains and heat losses, solar heat gain coefficient and U-value, of the PV-DSFs operating under different operation modes, were analyzed and compared.

5.1. Passive heating effect in Mode 1

The experimental study of the passive heating effect of the PV-DSF operating in Mode 1, as shown in Fig. 3(a),

was conducted from Jan. 5 to Jan. 7, 2013. The heat flux and various temperature profiles of the PV-DSF system are presented in Fig. 5. Fig. 6 presents the incoming solar radiation as well as the solar heat gain coefficient (SHGC) of the PV-DSF system. It is seen that although the maximum ambient temperature was below 20 °C on the sunny days of the coldest month in Hong Kong, the indoor temperature during office hours, was always above the air-conditioning design temperature. The highest indoor temperature reached 33 °C. These results suggest that the PV-DSF system operating in Mode 1 could serve as an effective passive heater during the daylight hours of a sunny winter's day. The high PV module temperature of up to 50 °C, resulted in the transfer of a large heat flux of about 180 W/m² from the PV modules to the indoor room. The average SHGC of the PV-DSF system operating in Mode 1 was about 0.19, a value which is lower than that of a DSF with a low-e coating (Chow et al., 2010).

Fig. 7 presents the cloudy day temperature profiles of the PV-DSF system operating in Mode 1. It is seen that on a cloudy day, such as occurred on Jan. 10, the indoor temperature did not reach the air-conditioning design temperature. Once the solar radiation intensity exceeded 300 W/m², such as on Jan. 12, the indoor temperature did reach the air-conditioning design temperature and met the space heating requirement. According to previous weather data, the solar radiation could exceed 300 W/m² for most of the daylight hours during the coldest month in Hong Kong. This indicates that the PV-DSF operating in Mode 1 could play an important passive heating role even in Hong Kong's coldest month.

5.2. Comparisons of thermal performance in Mode 2

The objective of Mode 2, shown in Fig. 3(b), is to compare the thermal performances of PV-DSFs operating under non-ventilated and naturally-ventilated conditions,

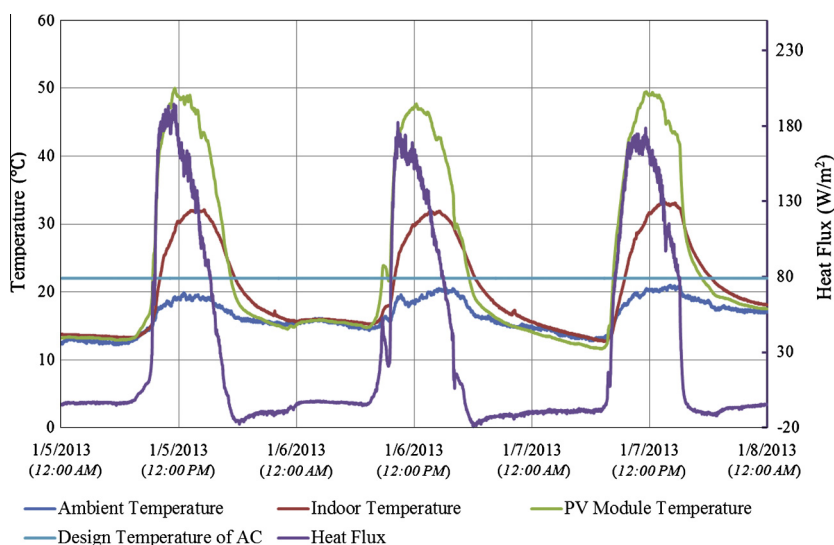


Fig. 5. The heat flux and various temperature profiles of PV-DSF operating in Mode 1.

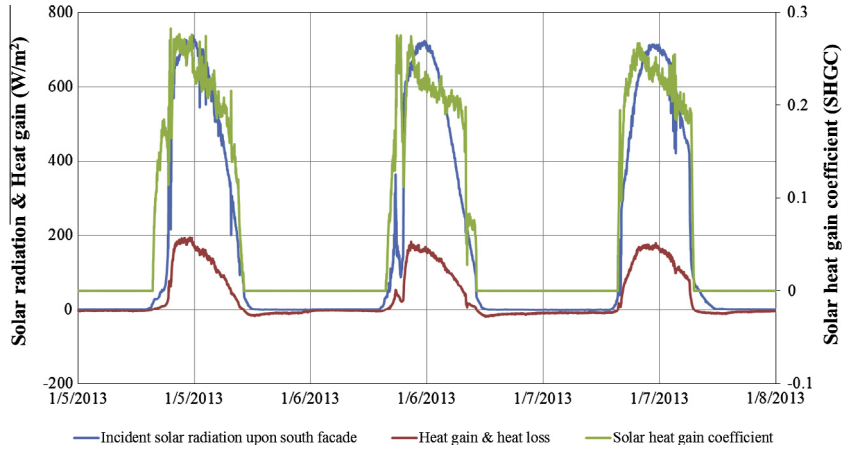


Fig. 6. The incident solar radiation and the SHGC of PV-DSF in Mode 1.

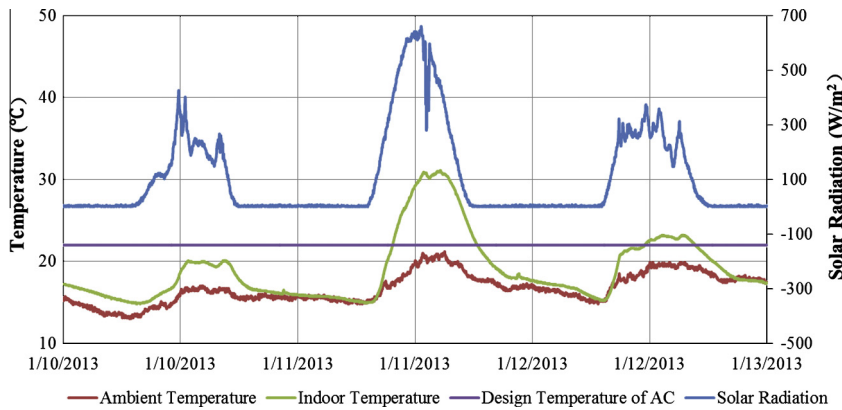


Fig. 7. The cloudy day temperature profiles of PV-DSF in Mode 1.

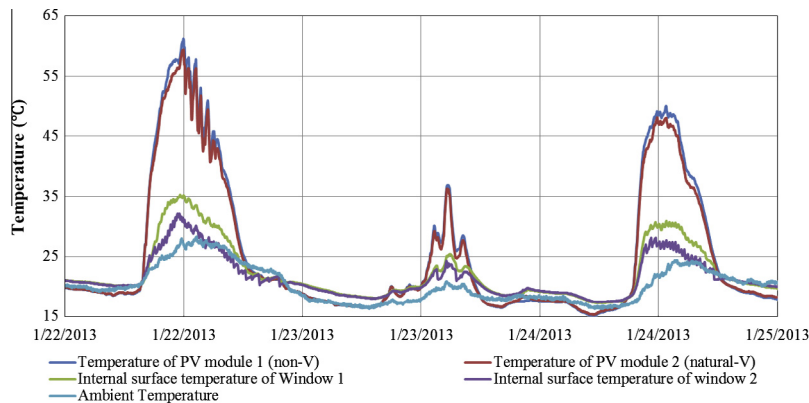


Fig. 8. The temperature profiles of PV-DSFs operating in non-ventilated and naturally-ventilated modes.

so as to explore the optimum operating modes for this system during different weather conditions.

The temperature profiles of PV-DSFs in non-ventilated and naturally-ventilated conditions are shown in Fig. 8. From Fig. 3(b), it is seen that in Mode 2, the inlet and outlet louvers of PV Module 1 are closed while the outlet louver of PV Module 2 is open. Thus, PV Module 1 operated under a non-ventilated condition while PV Module 2 oper-

ated under a naturally-ventilated condition. As shown in Fig. 8, the operating temperature of PV Module 1 is slightly higher than that of PV Module 2, while the maximum temperature difference between the internal surface temperatures of Window 1 and Window 2 reaches up to 3 °C on sunny days. The higher internal surface temperature of Window 1 resulted in higher convection heat flux from the non-ventilated PV-DSF to the interior of the

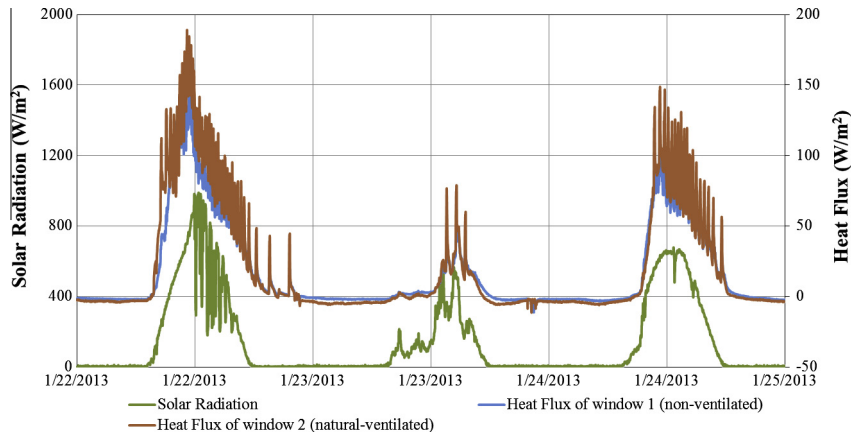


Fig. 9. Comparison of heat fluxes of PV-DSFs operating in non-ventilated and naturally-ventilated modes.

room. It is worth noting, however, that although the internal surface temperature of Window 1 is always higher than that of Window 2 during daytime, the heat flux from Window 2 to the indoor room is mostly higher than that of Window 1 in Fig. 9. The main reason was that the outlet louver above PV Module 2 was open and sunlight could penetrate the gaps between the louver grilles and thus directly transmit heat into the indoor room. This is also why the heat flux of Window 2 in Fig. 9 fluctuates periodically. This result suggests that an automatic louver continually adjusted according to the solar zenith angle should be introduced in the future design for this kind of ventilated PV-DSF, so as to reasonably regulate the daily solar radiation in different seasons. Specifically, the louver grilles should be adjusted, according to the solar zenith angle, to block the direct exposure to sunlight in summer in order to reduce solar heat gain while letting sunlight directly enter the indoor room in winter for meeting the requirements of natural lighting and space heating.

If the outlet louver of PV Module 2 is adjusted appropriately to avoid direct sunlight exposure, the heat flux from Window 2 to the interior of the room would be lower than that from Window 1, as shown in Fig. 9. Thus, it can be concluded that an optimally designed naturally-ventilated

PV-DSF has a lower PV module temperature and lower heat flux than those of a non-ventilated PV-DSF.

5.3. Comparisons of thermal performance in Mode 3

Fig. 10 presents the temperature profiles of PV-DSFs operating in ventilated and non-ventilated conditions. As shown in Fig. 3(c), the left PV-DSF system operates under non-ventilated condition, while that on the right operates under ventilated condition.

It was found that the operating temperature of PV Module 1 and the internal surface temperature of Window 1 were both noticeably higher than the respective values of PV Module 2 and Window 2. The maximum temperature differences between the two PV modules and the two windows were 6.3 °C and 5.7 °C, respectively. Similarly, and for the same reason given above in Section 4.2, the heat flux from the ventilated PV-DSF fluctuates periodically in Fig. 11. The average heat gain of the ventilated PV-DSF, however, was also lower than that of the non-ventilated PV-DSF, by about 10 W/m² on a sunny day.

The thermal performance of building envelopes, including window, external wall and facade, usually, can be quantified by the solar heat gain coefficient (SHGC or g-value)

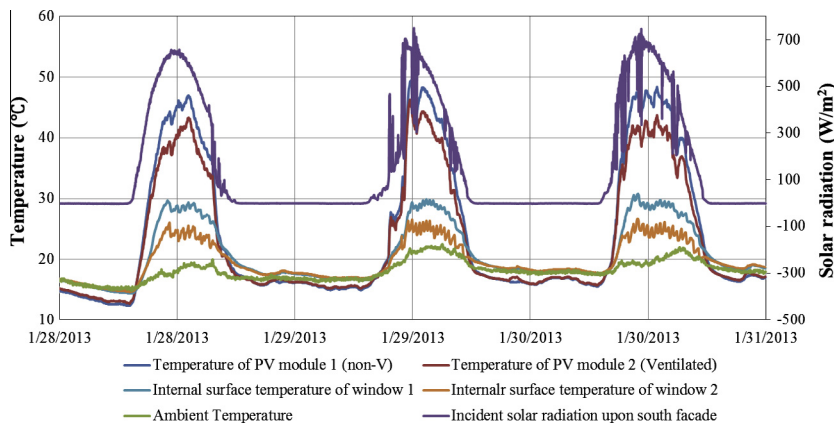


Fig. 10. The temperature profiles of PV-DSFs operating in ventilated and non-ventilated modes.

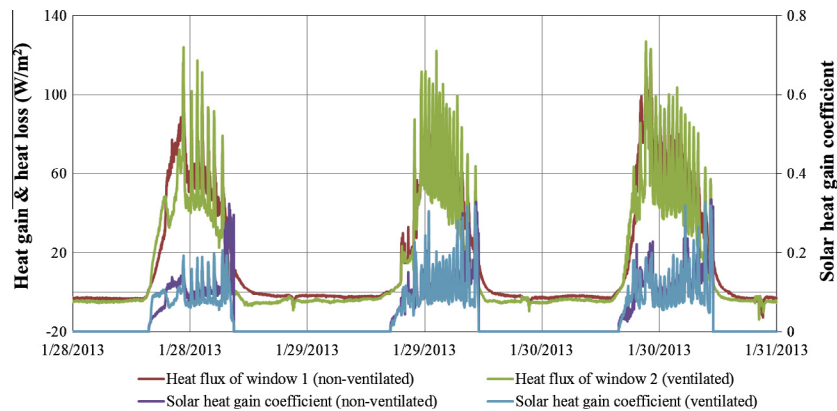


Fig. 11. Comparison of heat fluxes and SHGCs of PV-DSFs operating in ventilated and non-ventilated modes.

and U-value (Chow et al., 2010). As shown in Fig. 11, the average SHGC of the ventilated PV-DSF is about 0.1, while the average SHGC of the non-ventilated PV-DSF is about 0.13. The average SHGC of the naturally-ventilated PV-DSF is between these two values. These results indicate that the ventilated PV-DSF has the best thermal performance in terms of SHGC among the three operating conditions, and could reduce the solar heat gain by 30% more than the non-ventilated PV-DSF. Thus, the PV-DSF should operate in a ventilated mode so as to reduce solar heat gain as well as the PV module operating temperature in daytime during the summer. During the summer and at nighttime, the PV-DSF should operate under ventilated mode with the inward opening window open to enhance heat dissipation from the interior of the room. It is worth noting that even the average SHGC of the non-ventilated PV-DSF is lower by 40%, than that of a tinted-glass DSF with low-e coating (Chow et al., 2010). For heat loss performance, the average U-values of the non-ventilated, naturally-ventilated and ventilated PV-DSFs are found to be 3.4, 3.8 and 4.6, respectively. Thus the non-ventilated PV-DSF has the best performance in terms of reducing heat loss. Its U-value is higher than that of a DSF with low-e coating, but lower than that of a DSF filled with Argon (Chow et al., 2010). These results indicate that the PV-DSF should operate under a non-ventilated mode to reduce heat loss on a cloudy winter's daytime as well as at night during the winter.

Characteristically, Hong Kong, located in the subtropical climate zone, has warm winters and hot and humid summers. These climatic characteristics make the SHGC the dominant factor in the evaluation of the thermal performance of a facade. Thus, although the U-values of PV-DSFs operating under different ventilation modes are all higher than that of a low-e coating DSF, the PV-DSF is more suitable for Hong Kong because of the lower SHGC. This conclusion can be more generally extended to other tropical and subtropical climate zones. In addition, it is found that the PV modules temperatures are always lower than the ambient temperature by 1–2 °C at night, which may be attributed to the relatively high emissivity of PV modules.

5.4. Comparisons of thermal performance in Mode 4

Figs. 12 and 13 present the temperature profiles and heat fluxes of PV-DSFs operating in ventilated and naturally-ventilated conditions. As shown in Fig. 3(d), the left PV-DSF system operated under a naturally-ventilated condition and the right, under a ventilated condition. It was found that the respective operating temperature of PV Module 1 and the internal surface temperature of Window 1 were both higher than those of PV Module 2 and Window 2. The respective maximum temperature differences between the two PV modules and the two windows were 4.8 °C and 5 °C. The average heat gain of ventilated PV-DSF was also lower on sunny days than that of the naturally-ventilated PV-DSF, by about 6 W/m². However, this heat flux difference may be closely related to the ambient wind speed. From Fig. 12, it is seen that the ambient temperature and the internal surface temperature of Window 2 were similar on 2 Feb. At a moment such as this, the air-conditioning could be turned off and the PV-DSF allowed operate in ventilated mode with an open inward opening window for exchange of air with ambient air. In addition, at certain times of the year, the PV-DSF may operate in naturally-ventilated mode to balance heat loss and heat gain.

5.5. Optimum operation strategy

The thermal performance of PV-DSF operating under different modes has been analyzed and described in detail in the above sections. For an easy and intuitive comparison, the experimental results are summarized and presented in Table 4. It is seen that, compared with other PV-DSF operation modes, the ventilated mode not only reduces the heat gain rate and SHGC, but also reduces the indoor room temperature and that of the PV module. The PV module temperature decrease is beneficial in the enhancement of the PV module's energy conversion efficiency. However, the ventilated PV-DSF U-value is higher than that of non-ventilated and natural-ventilated modes, indicating that it has a poorer thermal insulation performance at night time in winter.

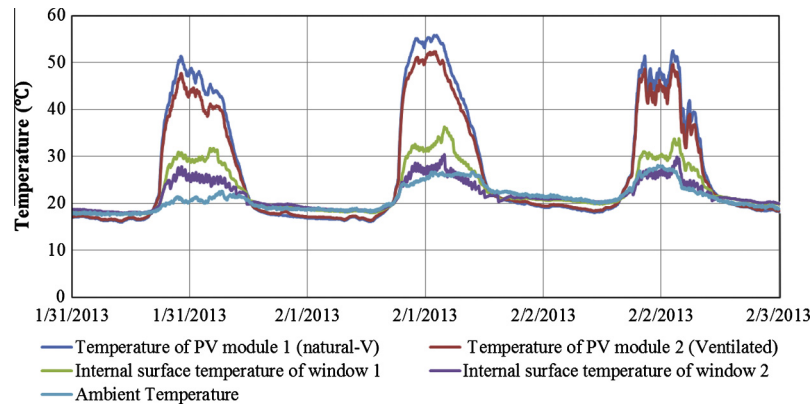


Fig. 12. The temperature profiles of PV-DSFs operating in ventilated and naturally-ventilated modes.

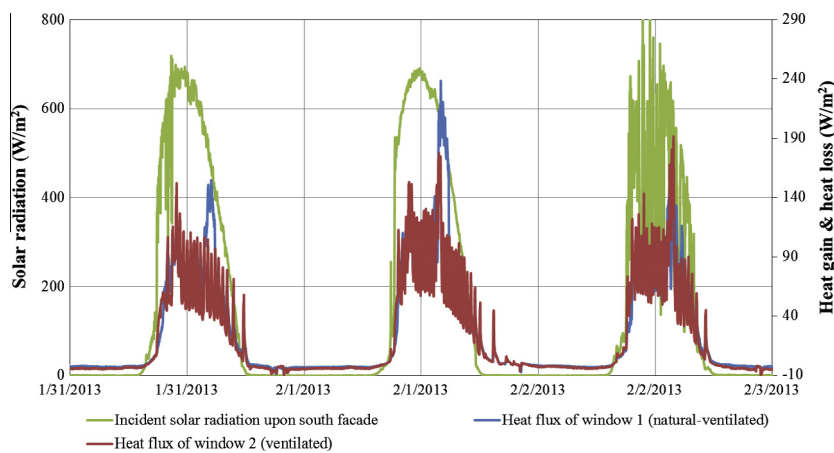


Fig. 13. Comparison of heat fluxes of PV-DSFs operating in ventilated and naturally-ventilated modes.

Table 4
Summary of the thermal performance of PV-DSF operating under different modes.

| Operation Modes | Mode 1 (5–7 Jan.) | Mode 2 (non-V vs. natural-V) (22–24 Jan.) | Mode 3 (non-V vs. V) (28–30 Jan.) | Mode 4 (natural-V vs. V) (31 Jan–2 Feb.) |
|--|-------------------|---|-----------------------------------|--|
| SHGC (9:00 AM–5:00 PM) | 0.19 | 0.15/0.13 ^a | 0.13/0.10 | 0.17/0.15 |
| U-value (5:00 PM–9:00 AM) | 5.9 | 3.2/3.6 | 3.4/4.6 | 3.8/4.7 |
| Indoor temperature, (°C) (9:00 AM–5:00 PM) | 28.3 | 26.9/24.7 ^b | 26.9/23.5 | 29.1/25.3 |
| PV module temperature, (°C) (9:00 AM–5:00 PM) | 40.4 | 38/36.7 | 39.3/35.8 | 43.9/41 |
| Heat gain, (W/m ²) (9:00 AM–5:00 PM) | 108.6 | 50/45 ^c | 53.3/42.1 ^c | 75.8/70.2 |

^a This SHGC has deducted the impact of sunlight penetration into the louvre.

^b The internal surface temperature of the inward-open window was adopted here.

^c This heat gain rate has deducted the impact of sunlight penetration into the louvre.

Based on the above experimental results, an optimum operation strategy for the PV-DSF is proposed as follows:

- (1) During the daytime hours of a sunny winter's day, the PV-DSF should operate in Mode 1, viz. to provide some passive heating. All inlet and outlet louvers should be closed and the inward opening windows should be opened.
- (2) During the daytime hours of a cloudy winter's day and also at nighttime during winter, the PV-DSF should operate in non-ventilated mode to reduce building heat loss through the facade.
- (3) During daytime hours in summer, the PV-DSF should operate in ventilated mode to enable reduction of solar heat gain as well as the operating temperature of the PV modules.

- (4) During nighttime hours in summer, the PV-DSF should operate in ventilated mode with inward opening windows left open to speed up heat dissipation from the interior of the room.
- (5) When the air-conditioning is turned off at certain times in spring and autumn, the PV-DSF may operate in ventilated mode with inward opening windows left open for the purpose of indoor air exchange.
- (6) At the other times of the year, the balance of heat loss and heat gain would be maintained by allowing the PV-DSF to operate in naturally ventilated mode.

6. Conclusions

Experiments and their results on the thermal behavior of a novel ventilated photovoltaic (PV) double-skin facade (DSF) system have been reported in this paper. This PV-DSF system can not only generate electricity in situ but also reduce the heat gains and heat losses through the building envelope. The beneficial effects of the ventilation duct were also visually demonstrated using infrared thermal imaging. It was found that the air temperature at the outlet louver of the PV-DSF was higher than that at the inlet louver by 2.2–2.3 °C. The thermal performance of PV-DSFs operating in different ventilation modes were analyzed and compared. The average solar heat gain coefficient (SHGCs) of the ventilated, naturally-ventilated and non-ventilated PV-DSFs were 0.1, 0.12 and 0.13, respectively. These experimental results indicate that the ventilated PV-DSF gives the best performance in terms of SHGC. Compared with a tinted-glass DSF with low-e coating, however, even the non-ventilated PV-DSF can reduce the SHGC by 40%. For heat loss performance, the average U-values of the ventilated, naturally-ventilated and non-ventilated PV-DSFs were 4.6, 3.8 and 3.4, respectively. Thus, the non-ventilated PV-DSF is the most effective in reducing heat loss. Although the U-values of PV-DSFs operating in different ventilation modes were all always higher than those of a low-e coating DSF, the PV-DSF is more suitable for buildings located in tropical and subtropical climate zones, such as found in Hong Kong and Singapore, due to its much lower SHGC. Based on the experimental results obtained under different operation modes, an optimum operation strategy for the PV-DSF was also proposed for maximizing its thermal energy efficiency under different weather conditions.

Acknowledgements

The authors appreciate the financial supports provided by the Innovation and Technology Commission of the Hong Kong Special Administrative Region (HKSAR) through the Innovation & Technology Fund (GHP/040/08GD) and the Hong Kong Polytechnic University through the grant 1-ZV6Z. The authors also thank Dr. Elaine Anson for polishing the written English.

References

- Chan, A.L.S., Chow, T.T., Fong, K.F., Lin, Z., 2009. Investigation on energy performance of double skin facade in Hong Kong. *Energy and Buildings* 41, 1135–1142.
- Charron, R., Athienitis, A.K., 2006. Optimization of the performance of double-facades with integrated photovoltaic panels and motorized blinds. *Solar Energy* 80, 482–491.
- Chow, T.T., Fong, K.F., He, W., Lin, Z., Chan, A.L.S., 2007. Performance evaluation of a PV ventilated window applying to office building of Hong Kong. *Energy and Buildings* 39, 643–650.
- Chow, T.T., Qiu, Z.Z., Li, C.Y., 2009a. Potential application of “see-through” solar cells in ventilated glazing in Hong Kong. *Solar Energy Materials and Solar Cells* 93, 230–238.
- Chow, T.T., Pei, G., Chan, L.S., Lin, Z., Fong, K.F., 2009b. A comparative study of PV glazing performance in warm climate. *Indoor and Built Environment* 18, 32–40.
- Chow, T.T., Li, C.Y., Lin, Z., 2010. Innovative solar windows for cooling-demand climate. *Solar Energy Materials and Solar Cells* 94, 212–220.
- Gratia, E., Herde, A., 2004. Optimal operation of a south double-skin facade. *Energy and Buildings* 36, 41–60.
- Gratia, E., Herde, A., 2007. Guidelines for improving natural daytime ventilation in an office building with a double-skin facade. *Solar Energy* 81, 435–448.
- Haase, M., Amato, A., 2006. Design considerations for double-skin facades in hot and humid climates. In: *Proceedings of the Sixth International Conference for Enhanced Building Operations*, Shenzhen, China, November 6–9, 2006.
- Han, J., Lu, L., Yang, H.X., 2010. Numerical evaluation of the mixed convective heat transfer in a double-pane window integrated with see-through a-Si PV cells with low-e coatings. *Applied Energy* 87, 3431–3437.
- Han, J., Lu, L., Peng, J.Q., Yang, H.X., 2013. Performance of ventilated double-sided PV facade compared with conventional clear glass facade. *Energy and Buildings* 56, 204–209.
- He, W., Zhang, Y.X., Sun, W., Hou, J.X., Jiang, Q.Y., Ji, J., 2011. Experimental and numerical investigation on the performance of amorphous silicon photovoltaics window in East China. *Building and Environment* 46, 363–369.
- Hong Kong Electrical and Mechanical Services Department, 2012. Hong Kong energy end-use data 2012. <http://www.emsd.gov.hk/emsd/e_download/pee/HKEEUD2012.pdf>
- Infield, D., Mei, L., Eicker, U., 2004. Thermal performance estimation for ventilated PV facades. *Solar Energy* 76, 93–98.
- Jiru, T.E., Tao, Y.X., Haghghat, F., 2011. Airflow and heat transfer in double skin facades. *Energy and Buildings* 43, 2760–2766.
- Manz, H., Frank, T., 2005. Thermal simulation of buildings with double-skin facades. *Energy and Buildings* 37, 1114–1121.
- Miyazaki, T., Akisawa, A., Kashiwagi, T., 2005. Energy savings of office buildings by the use of semi-transparent solar cells for windows. *Renewable Energy* 30, 281–304.
- Park, K.E., Kang, G.H., Kim, H.I., Yu, G.J., Kim, J.T., 2010. Analysis of thermal and electrical performance of semi-transparent photovoltaic (PV) module. *Energy* 35, 2681–2687.
- Peng, J.Q., Lu, L., Yang, H.X., Han, J., 2013. Investigation on the annual thermal performance of a photovoltaic wall mounted on a multi-layer facade. *Applied Energy*. <http://dx.doi.org/10.1016/j.apenergy.2012.12.026> (available online 01.09.13).
- Radhi, H., 2010. Energy analysis of facade-integrated photovoltaic systems applied to UAE commercial buildings. *Solar Energy* 84, 2009–2021.
- Safer, N., Woloszyn, M., Roux, J.J., 2005. Three-dimensional simulation with a CFD tool of the airflow phenomena in single floor double-skin facade equipped with a venetian blind. *Solar Energy* 79, 193–203.
- Wang, Y., Tian, W., Ren, J., Zhu, L., Wang, Q., 2006. Influence of a building's integrated-photovoltaics on heating and cooling loads. *Applied Energy* 83, 989–1003.

- Yun, G.Y., McEvoy, M., Steemers, K., 2007. Design and overall energy performance of a ventilated photovoltaic facade. *Solar Energy* 81, 383–394.
- Zhou, J., Chen, Y.M., 2010. A review on applying ventilated double-skin facade to buildings in hot-summer and cold-winter zone in China. *Renewable and Sustainable Energy Reviews* 14, 1321–1328.
- Zöllner, A., Winter, E.R.F., Viskanta, R., 2002. Experimental studies of combined heat transfer in turbulent mixed convection fluid flows in double-skin-facades. *International Journal of Heat and Mass Transfer* 45, 4401–4408.